27 May 2010, 4:30 pm - 6:20 pm

Behavior of Nailed Steep Slopes in Laboratory Shake Table Tests

Aniruddha Sengupta
IIT-Kharagpur, India

Debabrata Giri
IIT-Kharagpur, India


Fifth International Conference on
Recent Advances in Geotechnical Earthquake Engineering and Soil Dynamics
and Symposium in Honor of Professor I.M. Idriss
May 24-29, 2010 • San Diego, California

BEHAVIOR OF NAILED STEEP SLOPES IN LABORATORY SHAKE TABLE TESTS

Aniruddha Sengupta
Associate Professor, Dept. of Civil Engg.
IIT-Kharagpur, Kharagpur, W.B. 721302 (INDIA)

Debabrata Giri
Research Scholar, Dept. of Civil Engg.
IIT-Kharagpur, Kharagpur, W.B. 721302 (INDIA)

ABSTRACT

This paper presents results of laboratory shake table tests performed to study the dynamic behavior of nailed steep slopes. The surface displacements, settlement of the crest and the acceleration responses along with the behavior of the facing wall are examined during the tests. Two 18 cm high 60^0 and 70^0steep soil slopes reinforced with nine hollow aluminum nails placed in three rows are considered. Three strain gauges are glued to each nail to measure the tensile force developed in the nails. Four strain gauges are fixed at the center of the facing wall to measure the development of strains during shaking. The acceleration responses at the base and crest of the model slopes are monitored during the tests. The results clearly demonstrate advantage of a nailed slope over unreinforced slope. The failure surfaces observed in the shaking table tests are shallow and of rotational type. The nails oriented in horizontal direction are found to be more efficient. The nail forces and amplification of motion increase with the increase in slope angle and slope height. The amplitude of acceleration toward the outward slope direction is found to be larger than that toward the inward direction in all laboratory shaking tables tests.

INTRODUCTION

Soil nailing technique is one way of protecting slopes especially steep slopes against a catastrophic failure during earthquake. It provides the soil confinement and stabilizes entire slope. However the seismic resistance and the failure mechanism of nailed soil slope during an earthquake event is are not clearly understood and need to be investigated properly. Most of the literature on nailed soil structures emphasizes on the mechanism of reinforcement and the design of structures under static load only. Sakaguchi 1996, Koseki, et al. 1998, Matsuo, et al. 1998, in their studies have addressed the performance of geosynthetic reinforced retaining walls under seismic condition. The failure mechanisms for slopes under static loading have typically been extended to stability analysis of slopes under seismic loading using pseudo-static approach (Okabe 1924, Mononobe and Matsuo 1997), but the effect of seismic excitation on the failure pattern of slopes are not addressed. Bathurst and Alfaro 1997 also provided extensive reviews of seismic design and performance of geosynthetic reinforced walls, slopes and embankments. However, very few studies on the earthquake resistance and corresponding failure mechanisms of steep nailed slopes are available. Model tests in the laboratory can shed some lights on the performance of reinforced soil structures under dynamic loading condition. With this objective, a small scale shaking table has been developed at IIT, Kharagpur to study the reinforced embankment slopes under cyclic conditions. This paper presents the development of the shaking table and the results of the tests performed to study the dynamic behavior of steep soil slopes reinforced with nails. The surface displacements, settlement of the crest, strain behavior of the facing wall and the accelerations at the base and the crest of the slopes are measured during the tests.

DEVELOPMENT OF THE SHAKING TABLE SETUP

A new shaking table experimental setup is developed at the Indian Institute of Technology, Kharagpur by using a 2800 rpm and 7 HP DC motor. A slotted circular mild steel disc of 300 mm diameter and 20 mm thick is bolted to another circular disc of same size (used as a support to the slotted disc). The supported disc is connected to the shaft of motor. A steel crank shaft 500 mm long, 20 mm in diameter is connected to the slotted disc by bolts. The other end of the crank shaft is connected to a reciprocating rod, 500 mm long and 20 mm in diameter. The amplitude of a sinusoidal motion can be varied by changing the position of the crank shaft in the

calibrated slot of the disc. The other end of the reciprocating rod is connected to the shaking table's base plate. The reciprocating rod is kept in the horizontal position during the cyclic motion by a bracket support. The speed of the motor can be controlled from a panel board which essentially consists of an electrical variant.

The reinforced soil slope models are built in a 1.0 m x 0.90 m x 0.48 m (length x width x height) rectangular test box made up of 10 mm thick Perspex glass sheets to enable observation of deformations of the slopes from the sides. The sides of the box are fixed rigidly with steel angles to prevent any movement. The model box is fixed rigidly to the base plate of the shaking table with bolts. This base plate is fitted with very smooth wheels which slide in horizontal direction on two parallel rails. The three sides of the box are covered with 10 mm thick thermocol sheets to minimize the boundary effects. Sand particles are glued to the bottom surface of the model box to generate surface roughness, so that there is no slippage along the bottom surface during shaking. Acceleration responses during shaking are measured using Delta Tron Accelerometers (B & K Type 4507). Two accelerometers are mounted on the base plate of the shake table to measure the horizontal and the vertical vibrations. Another two accelerometers are fixed on the walls of the Perspex test box. One accelerometer is placed at the base of the slope and another one is placed at the crest of the model slope. The Bruel & Kjaer (B&K) Pulse 6.1 system (Type 3560c) sound and vibration meter is used for the data acquisitions. A schematic diagram of the experimental setup and the actual test setup are shown in Figure 1.

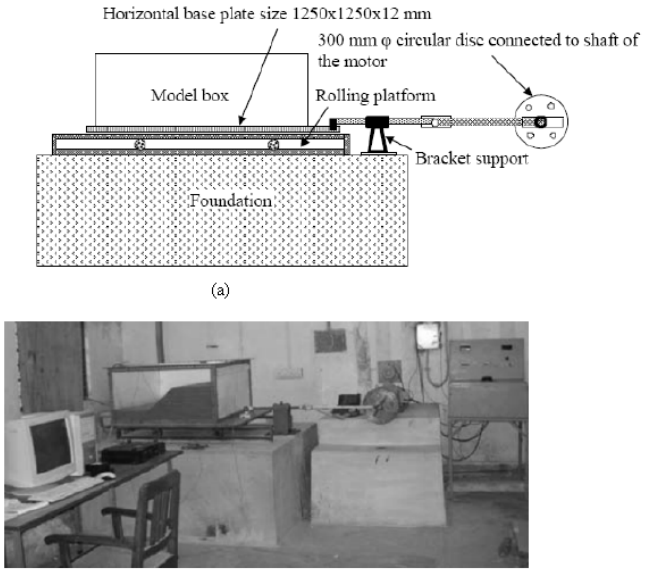

Fig. 1. (a) Schematic diagram of the experimental setup, and (b) Actual test setup.

The newly developed shaking table has a maximum stroke length of 150 mm and a peak frequency of 50 Hz. A system calibration has been done to check the performance of the experimental setup before starting the experimental work. The loading sequence used for the system calibration consists of a 10-sec of horizontal sinusoidal motions with peak acceleration of 0.1g at 3.85 Hz frequency and is shown in Figure 2. Note that the shaking table accelerates from rest to constant amplitude of 0.1g in 3.57 seconds. After this it is held constant at 0.1g for 10 seconds. The initial 3.57 seconds of motion are not shown in the figure. The responses of the accelerometers are also not shown for this initial 3.57 seconds. All the measurements are shown for the next 10 seconds of the input motion during which the amplitude of the sinusoidal motions is kept constant at 0.1g.

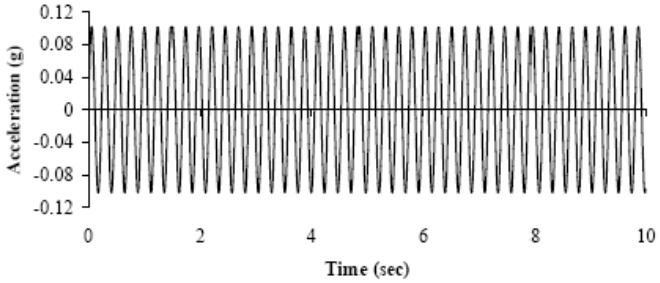

Fig. 2. 10 secs. of the input sinusoidal motions.

It is observed that no significant amplification of the system is registered during the loading and the system appears to behave linearly throughout the loading history. The responses of the accelerometers are found to be sinusoidal with predominant frequency of 3.85 Hz. This corresponds to a payload of 2 kN (weight of the base plate and the empty model box). The vertical vibration of the shaking base plate and the model box is also measured. The magnitude of the vertical vibration (0.0075g) of the base plate is very less as compare to the horizontal input motion and can not significantly affect the test results.

SPECIMEN PREPARATION & MATERIAL PROPERTIES

The soil used in this study is a local uniform medium sand (Kasai River sand). The grain size distribution of the sand is shown in Figure 3. It is classified as poorly graded sand (SP), according to the Unified Soil Classification System. The specific gravity of the sand is 2.7. The maximum dry unit weight, $\gamma_{d(max)}$, is 16.7 kN/m^3, and the minimum dry unit weight, $\gamma_{d(min)}$, is 14.03 kN/m^3. The uniformity coefficient (c_u) and coefficient of curvature (c_c) of the sand are found to be 2.84 and 0.87, respectively. In all the model tests, the bulk unit weight of the sand is maintained at 15.02 kN/m^3 and a relative density D_r of 60%. The drained triaxial shear test is performed on the soil samples to obtain the shear strength parameters. The cohesion and angle of friction are obtained from triaxial

(drained) test as 1.0 kPa and 32^0, respectively. Table 1 shows all other soil parameters. Before the construction of the model slopes, 3% water is added to the sand. The model slopes are constructed in the test box by compacting the cured sand up to the desired height by controlled-volume method. The pore water pressure development during the cyclic tests and development of suction pressure due to the addition of 3% water to the sand are found to be negligible (Lin et al., 2006) for all practical purposes and they do not significantly affect the stability of the slopes tested. Two geo-grid sheets are glued together and kept for more than 48 hours and then used as the facing wall. The properties of the facing wall are tabulated in Table 2. During the construction of the model slopes, the facing wall is used to maintain the slope surface at the desired angle.

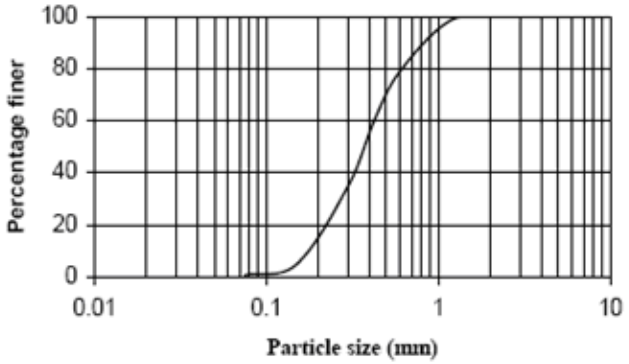

Fig. 3. The grain size distribution of the sand.

Table 1. Material Properties of the Sand.

Soil Properties	Value
Unit Weight γ at D_r= 60 %	15.02 kN/m^3
Cohesion, c	1.0 kPa
Friction Angle, φ	32^0
Static Shear Modulus, G	3.61 MPa
Static Young's Modulus, E	9.528 MPa
Dynamic Shear modulus, G_{dyn}	23.9 MPa
Dynamic Bulk modulus, K_{dyn}	36.3 Mpa

Table 2. Properties of Reinforcements & Facing Wall.

Reinforcement Properties	Value
Elastic modulus, E (at 2% strain)	134800GPa
Yield strength, T_y	5640 N/m^2
Compressive strength, T_c	0
Cross section area, A	201.1428 mm^2
Shear bond stiffness, K_{bond}	4.215 MPa
Density, ρ	2550 kg/m^3
Facing wall Properties	Value
Elastic modulus, E (coupon test)	7500.0 MPa
Tensile Yield Strength	23.45 MPa
Density	1850.0 kg/m^3

The performances of two 18 cm high slopes with slope angles of 60^0 and 70^0 are studied. In the first stage of the experimental program, the stability of the slopes without any reinforcements is investigated under the cyclic loading condition. In the second phase of the study, the performance of the same slopes reinforced with nails is studied. Each model slope is reinforced with nine numbers of hollow aluminum nails spaced at a constant vertical spacing of 6 cm and a horizontal spacing of 22 cm. The nails are anchored at right angle to the facing wall. Sand particles are glued to the surface of the nails to generate surface roughness. Three strain gauges of type BKCT-3 (resistance 119.2 ± 0.2 ohms, gauge factor: 1.92± 2% and gauge length 3 mm) are glued at various points of each nail to record local strains. The ratio of length of nail to slope height is maintained at 0.8 for all cases.

RESPONSES OF THE MODEL SLOPES

All the model slopes are subjected to the same base acceleration which consists of sinusoidal motions with constant peak amplitude of 0.1g and frequency of 3.85 Hz (Figure 2). This is the same motion for which the test setup is calibrated before. The side view of the failed unreinforced model slopes is presented in Figure 4. It is observed that the unreinforced 70^0 slope failed at a peak acceleration of 0.08g. The unreinforced 60^0 slope failed at a peak acceleration of 0.06g. The development of the sliding surface and the crest

settlement for the nailed slopes at the end of each test are shown in Figures 5 and 6.

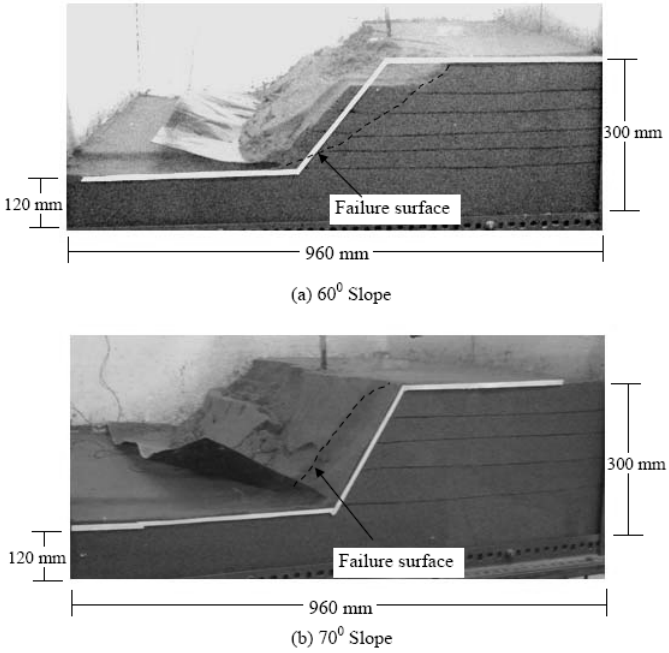

Fig. 4. Side views of the failed unreinforced slopes.

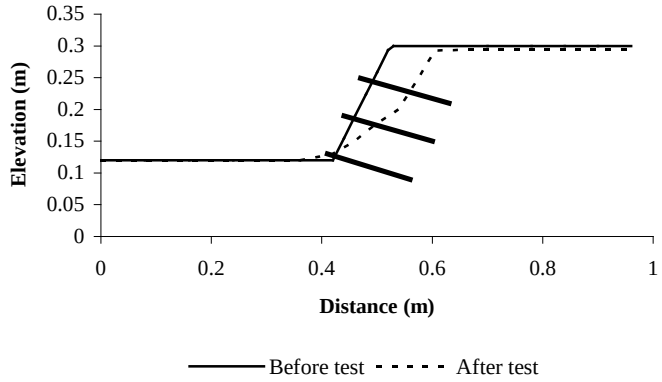

Fig.5. Deformations in the 60^o nailed slope.

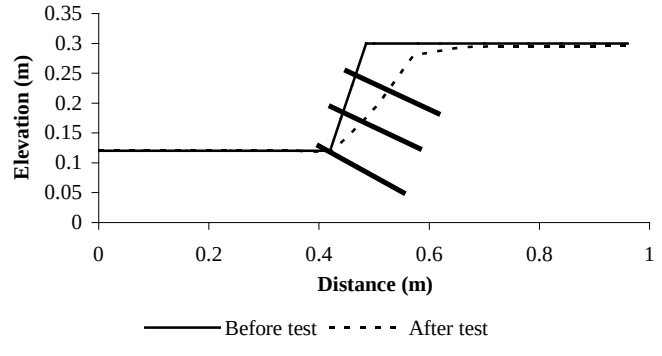

Fig.6. Deformations in the 70^o nailed slope.

The comparison of the behavior of the reinforced and unreinforced slopes in terms of crest settlement at the failure, peak acceleration and number of cycles to failure are given in Table 3. The number of cycles to slope failure as well as the peak acceleration that the reinforced slopes could sustain is much higher than the corresponding unreinforced slopes. The tests clearly demonstrate how the nail reinforcements have improved the dynamic stability of the steep slopes.

Table 3: Comparison of test results for unreinforced and reinforced slopes.

Slope Angle (^{0})	Maximum Crest Settlement (mm)		Peak Acceleration (g) at Failure		Number of Loading Cycles to Failure	
	With out Nail	With Nails	With out Nail	With Nails	With out Nail	With Nails
60	56	102	0.08	0.12	43	117
70	68	110	0.06	0.11	32	87

The photographs of the failed reinforced slopes are shown in Figures 7 and 8.

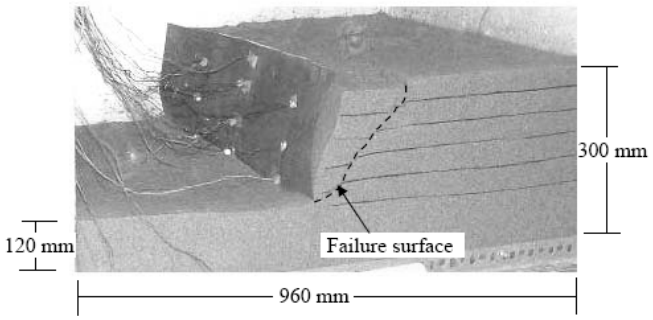

Fig. 7. Side view of the failed 60^0 slope at the end of the test.

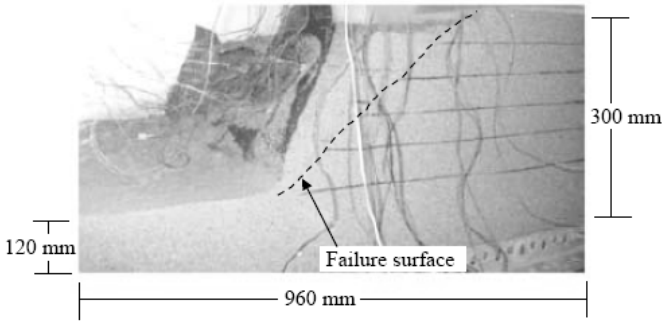

Fig. 8. Side view of the failed 70^0 slope at the end of the test.

In all the tests, a gap is developed between the soil slope and the facing wall before the final failure surface is appeared. The magnitude of the gap is found to be more at the crest of the slope. The developed gap at the crest is 102.5 mm for the 60^0 model slope. In case of the 70^0 slope, the gap at the crest is found to be 86 mm. The number of loading cycles (87) to failure is also less for the 70^0 model slope as compared to the 60^0 slope which failed at 117 loading cycles. The side views of the failed model slopes show that the facing wall for the 70^0 model slope has collapsed along with the retaining soil (Figure 8) while for the 60^0 slope model the facing wall, though separated out from the backfill reinforced soil, is still standing (Figure 7). In both the model slopes, toe failure is observed. The crest settlements are measured at the end of each test when the failure surface has developed completely. The crest settlement for the 70^0 model slope is 110 mm where as that for the 60^0 slope it is 102 mm. The area affected during failure is also more for the case of 70^0 model slope. The failure surface close to the crest is more or less circular. Some hairline tension cracks at the crest are also prominent. Less number of cracks is developed as the steepness of slope increases. This may be due to the fact that the slope becomes more unstable with the increase in slope angle and the sliding (failure) surface is shallower as the slope fails with less number of loading cycles.

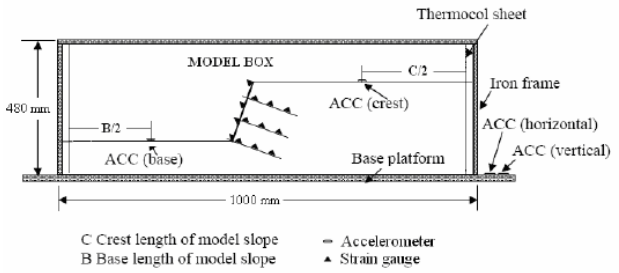

Fig. 9. Location of the accelerometers & location of strain gauges on the nails.

Four accelerometers are used to obtain acceleration responses during the tests. The positions of the accelerometers along with the position of nails with strain gauges for a model slope are shown in Figure 9. Two accelerometers are attached to the shaking table base platform to get horizontal and vertical input acceleration parameters, respectively. Another two accelerometers are placed at the centre of the base and the crest of the model slopes to measure amplification of the motion through the slope.

The applied horizontal motions at the base are same for all the cases and also confirmed to be same by the accelerometer located at the base of the slope. The crest acceleration histories of the model slopes are shown in Figure 10. The amplification of the motion (recorded crest acceleration/ input base acceleration) for the model slopes with 60^0 and 70^0 slope angles are 1.123 and 1.245, respectively. Table 4 summarizes the magnification of the acceleration through the slopes and the maximum crest settlement recorded in each test.

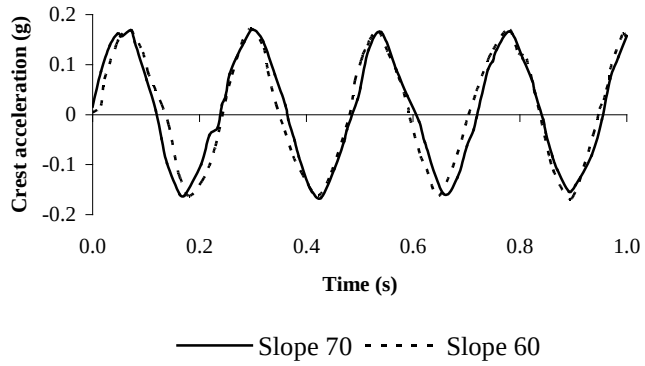

Fig. 10. Crest acceleration histories of the model slopes.

Table 4. Comparison of the crest settlement and amplification of motion at the crest.

Slope Angle (^{0})	Experimental Results	
	Maximum Crest Settlement (mm)	Amplification at Crest
60	102	1.123
70	110	1.245

Local strains corresponding to the loading cycles at different locations of each nail are measured with strain gauges. The reinforcement forces are calculated from the measured average strain using the load versus strain relationship determined from the tensile test on the aluminum nails. The elastic modulus of the aluminum nail is found to be 134.8 GPa in the laboratory by uniaxial tensile test. The variation of reinforcement force as calculated from the strain gauge readings is shown graphically in Figures 11 and 12.

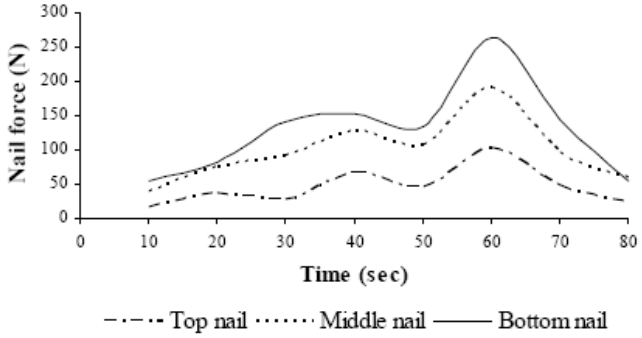

Fig. 11. Nail forces in the 60^0 model slope during shaking.

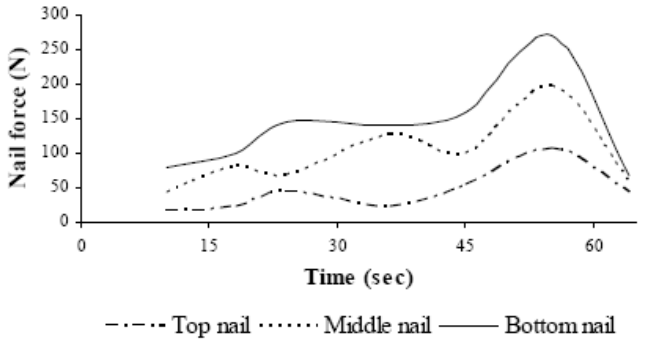

Fig. 12. Nail forces in the 70^0 model slope during shaking.

The above figures show that the induced nail forces varied nonlinearly with respect to the loading. The induced reinforcement (nail) forces are more for the steeper slope. The maximum induced force is 269.56 N for the 70^0 model slope as against 262.2 N for the 60^0 model slope. As the slope angle increases, the mass of the failure wedge also increases. This may be the season, why the induced force is more for the steeper slope. The top most nail doesn't generate significant force as compare to other nails. This is likely due to the lack of adequate soil confinement at the shallow depth. The maximum axial forces developed in the nails at the end of the prescribed motion in the shaking table tests are also compared with the values obtained by the pseudo-static analysis (Saran, 2005) and presented in Table 5.

Table 5. Comparison of maximum axial force (N) on nails.

Slope Angle (^{0})	Experimental Results			Pseudo-static Analysis		
	Top	Mid	Bottom	Top	Mid	Bottom
60	1.5	2.44	2.85	1.8	3.14	3.6
70	1.7	2.95	5.31	1.9	3.44	5.82

Four strain gauges are fixed at the mid width of the facing wall to obtain the lateral earth pressures on the wall during the motions. The positions of the strain gauges are 5 mm, 55 mm, 115 mm and 175 mm, respectively from the bottom of the slopes. The average variation of pressure with respect to the slope height is shown in Figure 13. A minimal pressure is obtained at the top of the facing wall. These induced pressures depend on the pseudo-static forces and mass of the failure wedge. The maximum pressure is obtained near about the centroid of the slopes. The maximum pressure is 8.5 kN/m^2 in the case of the 70^0 nailed slope. It is 7 kN/m^2 for the case of the 60^0 model nailed slope.

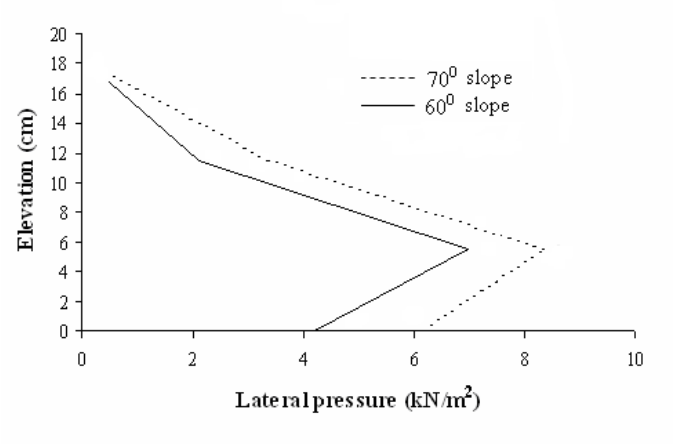

Fig. 13. Average lateral pressures on the facing wall.

CONCLUSIONS

Based on the present study on the dynamic behavior of nailed soil slopes, the following conclusions are drawn:

The failure surfaces appeared to be circular and confined to the zone near the slope surfaces. The observed failure surface is deeper for the steeper slope. The numbers of major cracks along with some hairline cracks are developed near the box boundary walls. Some intermediate cracks are also developed near the boundary and between major failure surfaces. It is likely that more than one set of failure surfaces might have developed during the laboratory shaking table tests. Number of cracks appeared to be less as the slope angle increases. With the increase in slope angle, the slope becomes more unstable and fails with less number of loading cycles. The mass movement and size of possible failure wedge decrease with decrease in loading cycles. This may be the reason for the development of less number of failure cracks in the steeper slope. The induced nail force varied nonlinearly with respect to loading cycles and the top nail doesn't generate significant force as compared to the other nails. This is likely due to the lack of adequate soil confinement. A minimal strain value is obtained at the top of the facing wall. The maximum strain is obtained near about the centroid of the slope. The magnification of the amplitude of the crest acceleration for steeper slope is more.

All the laboratory shaking table tests reported here, being done on small scale nailed embankment models, suffer from some limitations. The dilation of the sandy soil used in the tests is exaggerated and confining stresses around the nails are small as well. These may lead to under-performance of the soil nails in the tests. However, the tests give some fair indications

regarding the performance of the nailed embankments during a dynamic loading condition.

REFERENCES

Bathurst, R.J. and Alfaro, M.C. [1997]. "Review of seismic design, analysis and performance of geosynthetic reinforced walls, slopes and embankments", *Proceedings of the 3rd International Symposium on Earth Reinforcement*, Fukuoka, Japan, Balkama Rotterdam, Netherlands, pp. 887-918.

Koseki, J., Munaf, Y., Tatsuoka, F., Tateyama, M., Kojima, K. and Sato, T. [1998]. "Shaking and tilt table tests of geosynthetic reinforced soil and conventional type retaining walls", Geosynthetic International, Vol. 5, No. 1-2, pp. 73-96.

Lin, C.W., Shieh, C.L., Yuan, B.D., Shieh, Y.C., Liu, S.H. and Lee, S.Y. [2004]. "Impact of Chi-Chi earthquake on the occurrence of landslides and debris flows: example from the Chenyulan River watershed, Nantou, Taiwan", Engineering Geology, Vol. 71, No. 1-2, pp. 49-61.

Matsuo, O., Tsutsumi, T., Yokoyama, K. and Saito, Y. [1998]. "Shaking table tests and analyses of geosynthetic-reinforced soil retaining walls", Geosynthetic International, Vol. 5, No. 1-2, pp. 97-126.

Mononobe, N. and Matsuo, H. [1997]. "On the determination of earth pressure during earthquake", *Proceeding of the World Engineering Conference*, Tokyo, Japan, pp. 176.

Okabe, S. [1924]. "General theory on earth pressure and seismic stability of retaining wall and dam", Journal of the Japanese Society of Civil Engineering, Vol. 10, No. 6, pp. 1277-1324.

Sakaguchi, M. [1996]. "A study of the seismic behavior of geosynthetic-reinforced walls in Japan", Geosynthetic International, Vol. 3, No. 1, pp. 13-30.

Saran, S. [2005]. "*Reinforced soil and its engineering application*". I. K. International Pvt. Ltd, India.